論文 / 著書情報
Article / Book Information

Title	Individual transport of electrons through a chemisobed Au nanodot in Coulomb blockade electron shuttle
Authors	Yasuo Azuma,Norihiro Kobayashi,Simon Chorley,Jonathan Prance,Charles G. Smith,Daisuke Tanaka,Masayuki Kanehara,Toshiharu Teranishi,Yutaka Majima
Citation	J. Appl. Phys., Vol. 109, ,
発行日/Pub. date	2011, 1
公式ホームページ /Journal home page	http://jap.aip.org/
権利情報/Copyright	Copyright (c) 2011 American Institute of Physics

Individual transport of electrons through a chemisorbed Au nanodot in Coulomb blockade electron shuttles

Yasuo Azuma,[1,2] Norihiro Kobayashi,[1,2] Simon Chorley,[3] Jonathan Prance,[3] Charles G. Smith,[3] Daisuke Tanaka,[2,4] Masayuki Kanehara,[2,4] Toshiharu Teranishi,[2,4] and Yutaka Majima[1,2,5,a)]

[1]*Materials and Structures Laboratory, Tokyo Institute of Technology, Yokohama 226-8503, Japan*
[2]*CREST, Japan Science and Technology Agency (JST), Yokohama 226-8503, Japan*
[3]*Cavendish Laboratory, University of Cambridge, JJ Thomson Avenue, Cambridge CB3 0HE, United Kingdom*
[4]*Graduate School of Pure and Applied Sciences, University of Tsukuba, 1-1-1 Tennodai, Tsukuba, Ibaraki 305-8571, Japan*
[5]*Department of Printed Electronics Engineering, Sunchon National University, Sunchon 540-742, Republic of Korea*

(Received 22 September 2010; accepted 10 November 2010; published online 19 January 2011)

The individual transport of electrons through a chemisorbed Au nanodot is observed in accordance with a nanomechanical vibration of the Au nanodot on a cantilever at 86 MHz; the experimental setup consists of a scanning tunneling microscopy probe/vacuum/chemisorbed Au nanodot/cantilever. In the tunneling current-distance characteristics, a constant current of ef [where f is an eigenfrequency of the cantilever (86 MHz)] is observed as a plateau over a distance of 0.35 nm; this plateau is five times wider than that observed in the case of physisorbed Au nanodots. Coulomb blockade electron shuttle devices with chemisorbed Au nanodots are one of the candidates for current standard devices. © *2011 American Institute of Physics*. [doi:10.1063/1.3525833]

I. INTRODUCTION

Nanomechanical Coulomb blockade electron shuttle devices have attracted considerable attention owing to their unique characteristics, and they can be potentially employed in the field of nanoelectronics.[1–12] In nanometer-sized double-barrier tunneling structures, electron tunneling is restrained, and the number of electrons on Coulomb islands, n, is quantized because of a Coulomb blockade (CB). The polarity of electrons on a Coulomb island is highly dependent on the ratio of the tunneling resistance between the Coulomb island and the two reservoirs.[13] Gorelik *et al.* proposed a theory for electron transport due to mechanical oscillation of the Coulomb island, i.e., the shuttle mechanism.[1] They also predicted the self-excitation of the Coulomb island oscillation at the eigenfrequency of the center of mass of the system. This was attributed to the charging and discharging process on the Coulomb island, which occurred on the application of a dc voltage when the Coulomb island was movable and the ratio of the tunneling resistance between the Coulomb island and the two reservoirs was periodically inverted. When the Coulomb island shuttles, the probe tunneling current due to the electron shuttle is expressed as $I=gnef$, where g is the prefactor, n is the average number of electrons on Coulomb island, gn is the average number of electrons transported in each cycle, e is the unit charge, and f is the oscillation frequency of the Coulomb island. Under the ideal condition discussed by Gorelik *et al.*, i.e., $n=1$, an electron and a hole are individually transported per cycle of the Coulomb island oscillation, i.e., $gn=2$ and $I=2ef$.[1]

There are several trials for observing the tunneling current due to the electron shuttle, $I=ef$, in the door-bell structure fabricated by the Si process on the application of an rf signal.[3,10] In these systems, the Coulomb island is oscillated by the external rf signal. However, the tunneling current $I=ef$ has not been observed in these systems owing to the high capacitance of the sample structures.

We have demonstrated the electron shuttle phenomena in nanometer-sized double-barrier tunneling structures with a scanning vibrating probe,[13,14] and we have successfully observed the nanomechanical Coulomb blockade electron shuttle phenomena, $I=2ef$, in a cantilever-type Coulomb blockade electron shuttle device; the experimental setup consists of a scanning tunneling microscopy (STM) probe/vacuum/octanethiol {$[CH_3(CH_2)_7SH;C8S]$}-protected Au nanodots (C8S-Au nanodots)/Au–Ti-coated SiO_2 cantilever/vacuum/Si back electrode. The cantilever is oscillated by the application of an rf signal having a frequency (f) of 86 MHz.[15]

In our previous study, the C8S-Au nanodots, i.e., the Coulomb islands, were physically adsorbed on the Au–Ti-coated SiO_2 cantilever; however, they were not strongly anchored. It is well known that the electron tunneling phenomenon is highly dependent on the tunneling distance; for instance, the tunneling probability is approximately ten times greater when the tunneling distance is decreased by 0.1 nm in vacuum and by 0.2 nm in alkanethiol molecules.[26] Nanomechanical Coulomb blockade electron shuttle devices essentially exhibit mechanical perturbations in their own driving mechanisms; hence, excessive mechanical oscillation results in an excessive increment in the probability of the tunneling and co-tunneling phenomena. These conditions are

a)Author to whom correspondence should be addressed. Electronic mail: majima@msl.titech.ac.jp.

not suitable for observing the Coulomb blockade electron shuttle phenomena. Therefore, a strong anchoring between the Coulomb islands and the cantilever and fixed structures is crucial to the observation of a stable tunneling current due to the electron shuttle.

In this study, we demonstrate the individual transport of electrons through chemisorbed Au nanodots in accordance with the nanomechanical vibration of the Au nanodots, using a setup that consists of an STM probe/vacuum/chemisorbed Au nanodots/cantilever. We show the probe tunneling current-distance characteristics whereby the quantized current *nef* is observed on the application of an rf signal. We also discuss the stability of these characteristics in the case of nanomechanical Coulomb blockade electron shuttles with chemisorbed Au nanodots, as compared to those with physisorbed Au nanodots.

II. EXPERIMENTAL

The cantilever was fabricated on the Si substrate using the same technique as that described in the previous report.[15] A cantilever pattern (length $L=5\ \mu$m; width $w=2\ \mu$m) was etched via electron beam lithography on the SiO_2 (thickness $h=1\ \mu$m)/Si(100) (600 μm) substrate. After the formation of the resist pattern, a 40-nm-thick Ni layer was evaporated as a mask on the SiO_2 substrate via fluorine reactive ion etching (RIE), and the cantilever pattern was transferred by the lift-off process. The exposed SiO_2 was etched via fluorine RIE; next, the Ni mask was removed by using dilute nitric acid. The Si layer was then wet-etched by employing a mixture of KOH and isopropyl alcohol, thereby forming a free-standing cantilever structure. Au (80 nm)/Ti (1.5 nm) was evaporated on the substrate; then, annealing was carried out at 598 K for 45 min in order to flatten the Au layer.[16] The cantilever eigenfrequency was evaluated by using the probe tunneling current-frequency characteristics, as demonstrated previously; it was found to be approximately 85.7 MHz.[17]

The Au–Ti-coated SiO_2 cantilever was immersed in a 1 mM solution of C8S in ethanol for 12 h to form C8S self-assembled monolayers (SAMs). Immediately after the formation of the C8S SAMs, the cantilever was immersed in a 5 mM solution of decanedithiol $[HS(CH_2)_{10}SH;C10S2]$ in ethanol for 7 h in order to partially substitute C10S2 for C8S. It is important to note that if the SAMs are fabricated using a C8S/C10S2 mixture solution and not by the sequential procedure described above, the C10S2 molecules lie such that their axes are parallel to the surface.[18] After the formation of the C8S and C10S2 SAMs, the cantilever was immersed in a 0.5 mM solution of C8S-Au nanodots in chloroform for 7 h. Part of the C8S molecules surrounding the Au cores were substituted by the C10S2 molecules anchored on the cantilever; therefore, the C8S-Au nanodots were anchored by C10S2 molecules.[19,20] Finally, the cantilever was rinsed in chloroform in order to remove the physisorbed Au nanodots from Au–Ti-coated SiO_2 surface. As a result of these procedures, the Au nanodots directly anchored on the Au–Ti-coated SiO_2 cantilever via C10S2 remain intact. Using a transmission electron microscope image, the diameter of the Au core was estimated as 3.4 ± 0.4 nm.

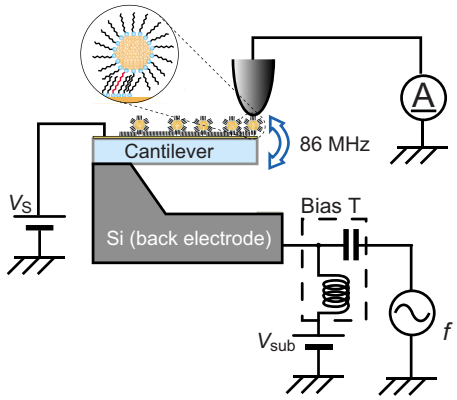

FIG. 1. (Color online) Experimental setup of cantilever-type nanomechanical Coulomb blockade electron shuttle, which consists of STM probe/vacuum/C8S protecting molecule/Au core/C10S2 molecule/Au–Ti-coated SiO_2 cantilever. The cantilever is oscillated at the eigenfrequency of 86 MHz by the application of an rf signal and V_{sub} to the Si back electrode below the cantilever. The amplitude of cantilever was 0.28 nm. The probe tunneling current between the STM probe and the Au–Ti-coated SiO_2 cantilever is measured by varying the distance between the probe and the cantilever at V_S.

Figure 1 shows the experimental setup of a cantilever-type nanomechanical single-electron shuttle device; it consists of a STM probe/vacuum/C8S protecting molecule/Au core/C10S2 molecule/Au–Ti-coated SiO_2 cantilever/vacuum/Si back electrode. The three terminals, i.e., the STM probe, Au–Ti-coated SiO_2 cantilever, and Si back electrode, were used for observing the probe tunneling current under the resonant vibration of the cantilever. The cantilever was oscillated by applying an rf signal (frequency: f) and a dc substrate voltage V_{sub} to the Si back electrode. The probe tunneling current between the STM probe and the Au–Ti-coated SiO_2 cantilever, I, was measured by varying the distance between the probe and the cantilever at the STM sample voltage V_S. The experiment was conducted using an ultrahigh vacuum STM (JEOL, JSPM-4500XT). In this procedure, the vacuum pressure was constantly maintained below 3×10^{-8} Pa, and the measurements were carried out at 100 K.

III. RESULTS AND DISCUSSION

Figure 2 shows the I-V_S characteristics in the double-barrier tunneling structure consisting of the STM probe/vacuum/C8S protecting molecule/Au core/C10S2 molecule/Au–Ti-coated SiO_2 cantilever, observed in the case of the marked C8S-Au nanodot without cantilever oscillation; the inset is an STM image of the nanodot. The Coulomb staircase is clearly observed. In this measurement, the dc voltage applied to the Si back electrode, V_{sub}, was the same as V_S so that the cantilever was not bent by an electrostatic force between itself and the Si back electrode.

According to the orthodox theory for a two-junction system, the tunneling processes across the junctions can be derived from a basic "golden rule" calculation; therefore, the theoretical I-V_S curve can be obtained on the basis of the following parameters. R_1, the tunneling resistance between the STM probe and the Au core; R_2, the tunneling resistance between the Au core and the Au–Ti-coated SiO_2 cantilever;

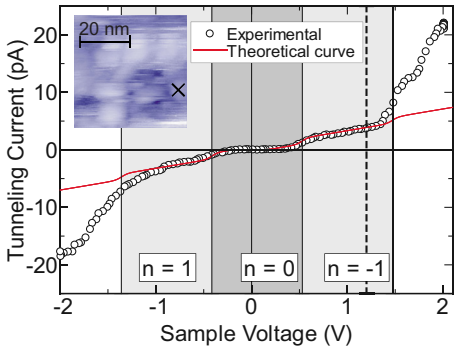

FIG. 2. (Color online) Probe tunneling current-sample voltage characteristics observed in the case of marked Au nanodot without rf signal. The theoretical Coulomb staircase (solid line) is also shown. Tunneling current-distance characteristics are observed at a sample voltage of $V_S=1.2$ V (shown by the vertical dashed line). The inset is an STM image (40×40 nm^2) of Au nanodots on the Au–Ti-coated SiO_2 cantilever.

C_1, the capacitance between the STM probe and the Au core; C_2, the capacitance between the Au core and the Au–Ti-coated SiO_2 cantilever; and Q_0, the fractional residual charge.[21–23] Figure 2 shows the theoretical curve with the following parameters: $R_1=260$ GΩ, $R_2=220$ MΩ, $C_1=0.17$ aF, $C_2=0.44$ aF, and $Q_0=0.05e$ C. The theoretical curve is in good agreement with the experimental $I-V_S$ characteristics in the voltage range of $-1.2<V_S<1.5$ V; the number of electrons on the C8S-Au nanodot, n, is evaluated as shown in Fig. 2. The tunneling resistance between the Au core and the Au–Ti-coated SiO_2 cantilever is estimated as $R_2=220$ MΩ. This value is closer to the tunneling resistance of C10S2 (630 MΩ) (Ref. 24) than to that of a C8S molecule, which is of the order of GΩ, as reported previously.[15,23,25–27] This result implies that the Au nanodots are not physisorbed on the C8S molecules but chemisorbed via the C10S2 molecules.

Figure 3 shows the experimentally determined relationship between I and the d (i.e., distance between the probe and the cantilever) on the application of an rf signal to the Si back electrode of cantilever-type nanomechanical Coulomb blockade electron shuttle devices with chemisorbed Au nanodots. The same sample and substrate voltages ($V_S=V_{sub}=1.2$ V) are applied, and the cantilever oscillates with an amplitude of 0.28 nm and an eigenfrequency of 86.0 MHz when a 6-dBm rf signal is applied to the Si back electrode.[17] Before the measurements were carried out, the set-point probe tunneling current was set to 5 pA. Then, the feedback circuit was turned off and the probe approached the cantilever. As can be seen in Fig. 3, a plateau is observed from 0.02 to 0.37 nm at a tunneling current ef of 13.8 pA. Despite the set-point probe tunneling current being set to 5 pA, the initial probe tunneling current increases to 13.8 pA; this value is maintained over a distance of 0.35 nm. Similar plateaus are also observed in the case of physisorbed Au nanodots (also shown in Fig. 3); however, the width of the plateau is 0.07 nm, i.e., approximately one fifth of that in the case of chemisorbed Au nanodots. Several plateaus and kinks are observed, at which the probe tunneling currents are integral multiples of $2ef=27.6$ pA. These phenomena were also observed in the case of cantilever-type nanomechanical Coulomb blockade electron shuttle devices with physisorbed Au nanodots, as reported previously.[15] Therefore, the plateau at the tunneling current of $2ef$ corresponds to individual electron and hole transport per cycle of the Coulomb island oscillation, whereas the other plateaus at which the probe tunneling currents are integral multiples of $2ef$ correspond to the single-electron shuttle phenomena due to the quantized number of Au nanodots.

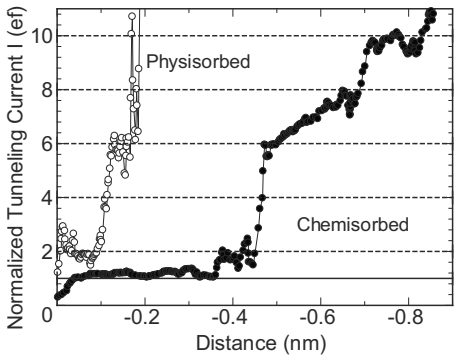

FIG. 3. Normalized probe tunneling current $I/(ef)$-distance characteristics in the cantilever-type nanomechanical Coulomb blockade electron shuttle devices with chemisorbed Au nanodots at $V_S=1.2$ V, cantilever oscillation amplitude of 0.28 nm (closed circles), and eigenfrequency of 86.0 MHz. $I/(ef)$-distance characteristics with physisorbed Au nanodots are also shown [open circles, as previously reported (Ref. 15)].

As discussed previously, the magnitude of the tunneling current at plateaus is an integral multiple of nef; this corresponds to single-electron shuttle transport due to the quantized number of Au nanodots, and it causes the current paths between the STM probe and Au–Ti-coated SiO_2 cantilever to be parallel.[15] The physisorbed Au nanodots were embedded in the Au–Ti-coated cantilever by employing the Langmuir–Blodgett technique; therefore, a number of nanodots were distributed in a close-packed manner. Hence, the number of Au nanodots contributing to single-electron shuttle transport increases when the change in distance is below 0.1 nm. On the other hand, chemisorbed Au nanodots were chemically anchored by C10S2, which partially exists on the Au–Ti-coated cantilever; hence, the density of Au nanodots is about 30 nanodots per 100×100 nm^2.[19] Thus, the density of chemisorbed Au nanodots is clearly less than that of physisorbed Au nanodots. In this case, the number of Au nanodots contributing to single-electron shuttle transport remains virtually unchanged because of their sparse density. Consequently, as shown in Fig. 3, the plateau width in the case of chemisorbed Au nanodots is 0.35 nm, i.e., five times greater than that in the case of physisorbed Au nanodots.

In the tunneling current-distance characteristics for the physisorbed Au nanodots (also shown in Fig. 3), the set point current (15 pA) was almost equal to $ef=13.8$ pA; hence, a plateau was observed at the tunneling current of $ef=13.8$ pA. However, a clear and stable plateau corresponding to ef was not observed in the case of cantilever-type nanomechanical Coulomb blockade electron shuttle devices with physisorbed Au nanodots. In the case of physisorbed Au nanodots, when the STM probe approaches the Au–Ti-coated cantilever and contacts a terminal of C8S protecting molecules, R_1 is ideally equal to R_2 because both the tunneling

resistances are attributable to C8S molecules. Based on this condition, the polarity of electrons on an Au core changes periodically with the cantilever oscillation. Therefore, the tunneling current due to the electron shuttle, $2ef$, is observed. In other words, electrons and holes are individually transported per cycle of the cantilever oscillation. On the other hand, in the case of chemisorbed Au nanodots, when the STM probe approaches the Au–Ti-coated cantilever and contacts a terminal of C8S protecting molecules, R_1 is greater than R_2 because R_1 and R_2 are attributable to C8S with a tunneling resistance of 3 GΩ and C10S2 with a tunneling resistance of 220 MΩ, respectively. Considering the initial difference in the tunneling resistances and the amplitude of the cantilever (0.28 nm), it should be impossible to invert the ratio of the tunneling resistance between an Au core and the two reservoirs when the cantilever is oscillated because of the initial difference between R_1 and R_2. Under this condition, the polarity of electrons on an Au core does not get inverted, and the number of electrons n periodically changes from $n=0$ to -1, not $n=1$. Therefore, a stable plateau is observed at a shuttle current of $ef=13.8$ pA, as shown in Fig. 3.

In Fig. 3, the plateau is observed at a shuttle current $ef=13.8$ pA in the range of $d=0.02-0.37$ nm; then the shuttle current increases to $2ef=27.6$ pA in the range of $d=0.37-0.45$ nm. This result implies that the ratio of tunneling resistances, i.e., R_1/R_2 is nearly one, and n periodically changes from $n=1$ to -1 around $d=0.37$ nm. If the protecting molecule of the Au core was only CS8 with a tunneling resistance of 3 GΩ, the distance at which $R_1/R_2=1$ would correspond to that at which the STM probe contacts a terminal of C8S protecting molecules. However, the protecting molecule between the Au core and Au–Ti-coated cantilever is C10S2 with a tunneling resistance of 220 MΩ; hence, the distance at which $R_1/R_2=1$ does not correspond to that at which the STM probe contacts a terminal of C8S molecules. Moreover, the STM probe should slightly penetrate into the C8S protecting molecules because the tunneling resistance of C8S is greater than that of C10S2. Note that in the case of chemisorbed Au nanodots, the shuttle current $2ef$ due to individual electron and hole transport is observed in the range of $0.45-0.37=0.08$ nm, which nearly corresponds to the range in which $2ef$ is observed in the case of physisorbed Au nanodots, i.e., 0.07 nm.[15] Under both these conditions, the STM probe touches and sometimes penetrates into the C8S protecting molecule. This physical contact disturbs the sample conditions and might result in an unstable shuttle current. Therefore, the shuttle current of $2ef$ is observed in a relatively small distance of below 0.1 nm.

On the other hand, although the length of the C8S molecule (1.24 nm) is smaller than that of the C10S2 molecule (1.59 nm), the tunneling resistance of C8S is greater than that of C10S2. Therefore, in the asymmetric structure of STM probe/vacuum/C8S protecting molecule/Au core/C10S2 molecule/cantilever, a condition of $R_1>R_2$ should be maintained over a large range of d without touching the C8S protecting molecule, as compared to the symmetric structure of STM probe/vacuum/C8S protecting molecule/Au core/C8S molecule/cantilever. Although the polarity of the electrons on an Au core does not get inverted and individual electron and hole transport is not observed, the stable shuttle current ef is observed over a large distance of 0.35 nm because of this asymmetric and chemisorbed structure.

IV. CONCLUSIONS

We demonstrated individual electron transport through a chemisorbed Au nanodot under nanomechanical vibration of the Au nanodot on a cantilever; the experimental setup used consists of a STM probe/vacuum/C8S protecting molecule/Au core/C10S2 molecule/cantilever. In the probe tunneling current-distance characteristics, a constant tunneling current ef due to the nanomechanical Coulomb blockade electron shuttle was observed over a distance of 0.35 nm for chemisorbed Au nanodots; this distance is five times greater than that for physisorbed Au nanodots. From these results, we conclude that Coulomb blockade electron shuttle devices with chemisorbed Au nanodots are one of the candidates for current standard devices.

ACKNOWLEDGMENTS

This study was partially supported by a Grant-in-Aid for Scientific Research on Innovative Areas (Grant No. 20108011, π-Space) from the Ministry of Education, Culture, Sports, Science and Technology (MEXT), Japan; Grant-in-Aid for Scientific Research (A) (Grant No. 19205016) from MEXT, Japan (T.T.); the Global COE Program of "Photonics Integration-Core Electronics," MEXT; Collaborative Research Project of Materials and Structures Laboratory, Tokyo Institute of Technology; the World Class University (WCU) program through the Ministry of Education, Science, and Technology of Korea (R31-10022), and EPSRC, UK.

[1] L. Y. Gorelik, A. Isacsson, M. V. Voinova, B. Kasemo, R. I. Shekhter, and M. Jonson, Phys. Rev. Lett. **80**, 4526 (1998).
[2] H. Park, J. Park, A. K. L. Lim, E. H. Anderson, A. P. Alivisatos, and P. L. McEuen, Nature (London) **407**, 57 (2000).
[3] A. Erbe, C. Weiss, W. Zwerger, and R. H. Blick, Phys. Rev. Lett. **87**, 096106 (2001).
[4] D. V. Scheible and R. H. Blick, Appl. Phys. Lett. **84**, 4632 (2004).
[5] Y. Xue and M. A. Ratner, Phys. Rev. B **68**, 235410 (2003).
[6] R. G. Knobel and A. N. Cleland, Nature (London) **424**, 291 (2003).
[7] M. D. LaHaye, O. Buu, B. Camarota, and K. C. Shwab, Science **304**, 74 (2004).
[8] A. D. Armour, M. P. Blencowe, and Y. Zhang, Phys. Rev. B **69**, 125313 (2004).
[9] Y. Majima, Y. Azuma, and K. Nagano, Appl. Phys. Lett. **87**, 163110 (2005).
[10] D. R. Koenig, E. M. Weig, and J. P. Kotthaus, Nat. Nanotechnol. **3**, 482 (2008).
[11] G. A. Steele, A. K. Hüttel, B. Witkamp, M. Poot, H. B. Meerwaldt, L. P. Kouwenhoven, and H. S. J. van der Zant, Science **325**, 1103 (2009).
[12] R. Taranko, M. Wiertel, P. Parafiniuk, and E. Taranko, Vacuum **83**, S169 (2009).
[13] K. Nagano, A. Okuda, and Y. Majima, Appl. Phys. Lett. **81**, 544 (2002).
[14] Y. Azuma, M. Kanehara, T. Teranishi, and Y. Majima, Phys. Rev. Lett. **96**, 016108 (2006).
[15] Y. Azuma, T. Hatanaka, M. Kanehara, T. Teranishi, S. Chorley, J. Prance, C. G. Smith, and Y. Majima, Appl. Phys. Lett. **91**, 053120 (2007).
[16] K. Sasao, Y. Azuma, N. Kaneda, E. Hase, Y. Miyamoto, and Y. Majima, Jpn. J. Appl. Phys., Part 2 **43**, L337 (2004).
[17] Y. Azuma, S. Chorley, J. Prance, C. G. Smith, and Y. Majima, Jpn. J. Appl. Phys., Part 1 **46**, 3152 (2007).
[18] K. Kobayashi, T. Horiuchi, H. Yamada, and K. Matsushige, Thin Solid Films **331**, 210 (1998).

[19]X. Li, Y. Yasutake, K. Kono, M. Kanehara, T. Teranishi, and Y. Majima, Jpn. J. Appl. Phys. **48**, 04C180 (2009).
[20]S. Hattori, S. Kano, Y. Azuma, and Y. Majima, J. Phys. Chem. C **114**, 8120 (2010).
[21]D. V. Averin and K. K. Likharev, in *Mesoscopic Phenomena in Solids*, edited by B. L. Altshuler, P. A. Lee, and R. A. Webb (Elsevier, Amsterdam, 1991).
[22]A. E. Hanna and M. Tinkham, Phys. Rev. B **44**, 5919 (1991).
[23]H. Zhang, Y. Yasutake, Y. Shichibu, T. Teranishi, and Y. Majima, Phys. Rev. B **72**, 205441 (2005).
[24]B. Xu and N. J. Tao, Science **301**, 1221 (2003).
[25]L. A. Bumm, J. J. Arnold, T. D. Dunbar, D. L. Allara, and P. S. Weiss, J. Phys. Chem. B **103**, 8122 (1999).
[26]Y. Yasutake, Z. Shi, T. Okazaki, H. Shinohara, and Y. Majima, Nano Lett. **5**, 1057 (2005).
[27]D. J. Fuchs and P. S. Weiss, Nanotechnology **18**, 044021 (2007).